The Functions of Crystallizable Ethylene-Propylene Copolymers in the Formation of Multiple Phase Morphology of High Impact Polypropylene

Cuiyan Tong,[1,2] Yang Lan,[2,3] Ye Chen,[1] Yong Chen,[1] Decai Yang,[1] Xiaoniu Yang[1]

[1]*State Key Laboratory of Polymer Physics and Chemistry, Changchun Institute of Applied Chemistry, Chinese Academy of Sciences, Changchun 130022, People's Republic of China*
[2]*Faculty of Chemistry, Northeast Normal University, Changchun 130024, People's Republic of China*
[3]*Staff Room of Inorganic Chemistry, School of Pharmaceutical Engineering, Shenyang Pharmaceutical University, Wen Hua Road No. 103, Shenyang, Liaoning 110016, People's Republic of China*

Received 11 February 2011; accepted 4 April 2011
DOI 10.1002/app.34609
Published online 15 August 2011 in Wiley Online Library (wileyonlinelibrary.com).

ABSTRACT: The functions of crystallizable ethylene-propylene copolymers in the formation of multiple phase morphology of high impact polypropylene (hiPP) were studied by solvent extraction fractionation, transmission electron microscopy (TEM), selected area electron diffraction (SAED), nuclear magnetic resonance (^{13}C-NMR), and selected reblending of different fractions of hiPP. The results indicate that hiPP contains, in addition to polypropylene (PP) and amorphous ethylene-propylene random copolymer (EPR) as well as a small amount of polyethylene (PE), a series of crystallizable ethylene-propylene copolymers. The crystallizable ethylene-propylene copolymers can be further divided into ethylene-propylene segmented copolymer (PE-*s*-PP) with a short sequence length of PE and PP segments, and ethylene-propylene block copolymer (PE-*b*-PP) with a long sequence length of PE and PP blocks. PE-*s*-PP and PE-*b*-PP participate differently in the formation of multilayered core-shell structure of the dispersed phase in hiPP. PE-*s*-PP (like PE) constructs inner core, PE-*b*-PP forms outer shell, while intermediate layer is resulted from EPR. The main reason of the different functions of the crystallizable ethylene-propylene copolymers is due to their different compatibility with the PP matrix. © 2011 Wiley Periodicals, Inc. J Appl Polym Sci 123: 1302–1309, 2012

Key words: high impact polypropylene; chain structure; crystallizable ethylene-propylene copolymers; phase morphology; multilayered core-shell structure

INTRODUCTION

High impact polypropylene (hiPP) produced by a multistage polymerization process is a type of complex multicomponent blending system, consisting of a polypropylene (PP) matrix, amorphous ethylene-propylene random copolymer (EPR), crystallizable ethylene-propylene copolymers, and a small amount of polyethylene (PE) homopolymer.[1–10] The interchain continuity and intrachain polydispersity are two characteristics of the copolymers. However, thus far, the understanding of crystallizable ethylene-propylene copolymers is widely contradictory. It seems that there is no doubt regarding the existence of ethylene-propylene segmented copolymers (PE-*s*-PP) with short sequence length of PP and PE segments in hiPP. However, the view of ethylene-propylene block copolymer (PE-*b*-PP) with long crystallizable PP and PE sequences is still controversial. Some researchers believe that the ethylene-propylene block copolymer can be formed during the second stage of the copolymerization in the production of hiPP,[6,8,10] whereas other research groups believe that the possibility of forming an ethylene-propylene diblock copolymer is questionable.[11,12] The structure similarity between the block copolymer and PE/PP blend as well as the poor purity of the block copolymer may be the main factors that affect identification of the block copolymer. In addition, the different sources of the materials should be another reason giving rise to the controversy since different methods of polymer synthesis may result in intrinsic structural difference of the materials.

The complex chain structure of hiPP must result in a complicated multiple phase morphology, whereas the multiple phase morphology is the key factor that makes the material possess excellent mechanical properties, with both high rigidity and high toughness.[2,3,9,13–15] It is generally believed that the dispersed phase in hiPP exhibits a core-shell structure with PE core and EPR shell.[16–19] This core-shell structure has proven to be efficient for the toughness–rigidity balance of the material. However,

Correspondence to: C. Tong (cytong@ciac.jl.cn).
Contract grant sponsor: Fundamental Research Funds for the Central Universities; contract grant number: 09QNJJ016

the understanding of the phase morphology of hiPP is far from perfect. Although one can obtain some information about the phase structure of hiPP bulk with the help of cryoultramicrotomy, staining, and surface etching techniques,[2,3,5,9,13–19] it is very difficult to gain the structural details of the phase morphology of the material. The corresponding relationship between the complicated chain structure and phase morphology has not been completely established. Especially, the effect of crystallizable ethylene-propylene copolymers on the formation of the multiple phase structure has not been clearly revealed to date. There is no report about the role of ethylene-propylene segmented copolymer with short length of ethylene and propylene sequences in the multiple phase morphology formation. Although one does not doubt that the ethylene-propylene block copolymer (or ethylene-propylene segmented copolymer with long sequence length of PE and PP segments, as mentioned in some literature) can be considered a compatibilizer enhancing the interface adhesion between the PP matrix and the EPR dispersed phase,[6,7,17] direct evidence of the distribution of the block copolymer in the interface is still lacking.

More recently, a multilayered core-shell structure of the dispersed phase of hiPP in both the bulk and the solution-cast film was observed for the first time in our work.[20,21] However, because of the small size of the dispersed phase and subsequent limitations of the current characterization methods, the structural details of the multilayered core-shell structure have not been completely understood. The objective of this study is to examine the functions of crystallizable ethylene-propylene copolymers (including both PE-*s*-PP and PE-*b*-PP) in the formation of the multilayered core-shell structure of the dispersed phase in hiPP on the basis of precise characterization of the chain sequence structure and to establish a relationship between chain structure, phase morphology, and mechanical properties of the material.

EXPERIMENTAL

Materials

The hiPP sample used in this work is a commercial product in pellet form (AW191, made in Singapore), synthesized in a multistage gas/gas polymerization process. The flexible modulus of the material is 0.989 GPa, and the notched Izod impact strength at 23 and −20°C are 205 and 79.6 J/m, respectively. The ethylene content is 19.8 mol %, as measured by ^{13}C-NMR.

Sample preparation

Four fractions of hiPP were prepared by successive solvent extraction fractionation. hiPP was completely dissolved in xylene at 130°C, and then, the solution was gradually cooled to room temperature. The precipitate was separated from the solution by filtration. Solvent in the remaining clear solution was evaporated, and a rubbery component was obtained as fraction F_a. The filtered precipitate was extracted successively by xylene at 80 and 100°C, respectively, the dissolved components were obtained as fractions F_b and F_c, whereas the undissolved part at 100°C was obtained as fraction F_d. The weight contents of the fractions were listed in Table I.

TABLE I
Contents of Fractions of hiPP

Fractions	F_a (RT)	F_b (80°C)	F_c (100°C)	F_d (>100°C)
Contents (wt %)	25.7	4.8	6.7	62.8

Thin films of hiPP and its fractions were prepared by casting 0.1 wt % xylene solution of the samples onto a carbon-coated mica surface at a temperature range of 100–130°C. After solvent evaporation, the films were cooled to room temperature and then vacuum-dried at the temperature for 24 h. Thin sections of the bulk sample were prepared by cryoultramicrotomy of the hiPP pellet with a Leica Ultracut R microtome (Vienna, Austria) operated at −80°C and a cutting speed of 1 mm/s.

Transmission electron microscopy (TEM)

For TEM observation, the thin films were transferred onto the surface of water and then collected on copper grids. A JEOL 1011 transmission electron microscope operated at 100 kV was used. Bright field (BF) electron micrographs were obtained by defocusing the objective lens. The camera length of the electron diffraction measurement was calibrated with Au.

RESULTS AND DISCUSSION

Composition and chain structure identification of hiPP fractions

To determine the functions of crystallizable ethylene-propylene copolymers in the formation of multiple phase morphology of hiPP, we must precisely identify the composition and chain structure of the material first, on the basis of fractionation. Generally, ^{13}C-NMR, FTIR, WAXD, and DSC have been combined to measure chain structure of fractionated samples of hiPP. However, since each fraction is not a pure single component and these methods generally give an average result, it is difficult to distinguish some subtle structural differences. In this work, in conjunction with ^{13}C-NMR analysis, transmission electron microscopy (TEM) and selected electron diffraction (SAED) techniques have been

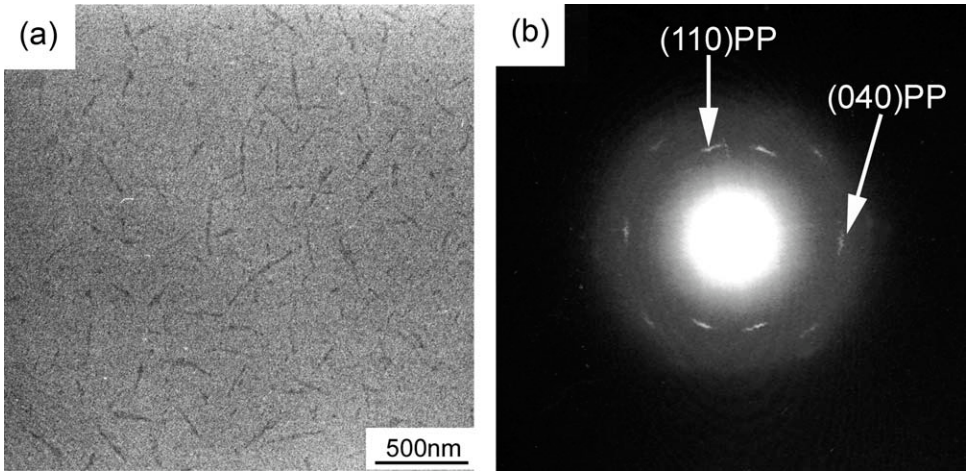

Figure 1 (a) TEM BF image of a solution-cast film of fraction F_a of hiPP; (b) SAED pattern of gray lines in (a).

effectively used for the first time to characterize the composition and chain structure of various fractions of hiPP.

Figure 1(a) displays a TEM BF electron micrograph of a solution-cast film of fraction F_a, which is dissolved in xylene at room temperature. Clearly, in addition to a small amount of dispersed gray lines, no typical morphological feature could be observed in the thin film of F_a, and combining with the results of NMR (in later part), we conclude that this fraction should be mainly composed of EPR. Election diffraction result of the gray lines [Fig. 1(b)] confirms that the gray lines are α-form PP crystals.

Figure 2(a) shows TEM BF image of a solution-cast film of fraction F_b, which is soluble in xylene at 80°C. In addition to loosely distributed PP crystals (the gray lines), there are some larger dark regions. Unambiguously, the strong contrast of the dark regions results from PE crystals. Selected area electron diffraction (SAED) of the dark regions exhibit two kinds of different diffraction patterns. One is typical orthorhombic reflections of (110) and (200) planes of PE crystals [Fig. 2(b)], which indicates the existence of some PE homopolymer in F_b. The other shows, in addition to (110) and (040) reflections of PP crystals, a set of six symmetric reflection spots with d spacing of 4.22 Å [Fig. 2(c)], which coincides well with the d value (4.33 Å) of the hexagonal crystal form of PE.[22] The symmetric six reflection spots are attributed to (100) reflection of hexagonal phase of PE, which was recently found in ethylene-propylene copolymers.[23–26] The explanation proposed in the literature for the formation of PE hexagonal phase at atmospheric pressure is that the defects in the form of side groups stabilize the PE hexagonal phase at ambient conditions. The result implies that the dark regions in fraction F_b which produce hexagonal reflection of PE should consist of crystallizable ethylene-propylene copolymer.

Figure 3(a) is the TEM BF electron micrograph of a solution-cast film of fraction F_c, which is the soluble fraction in xylene at 100°C. The dispersed dark regions with strong contrast represent PE crystalline phase, while the gray areas with weak contrast are

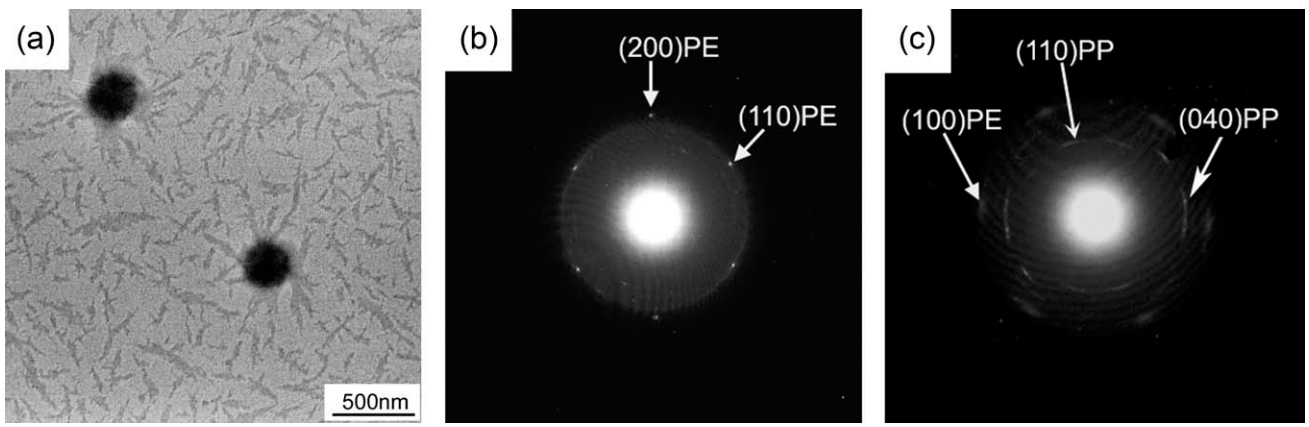

Figure 2 (a) TEM BF image of a solution-cast film of fraction F_b of hiPP; (b), (c) SAED patterns of different dark regions in (a).

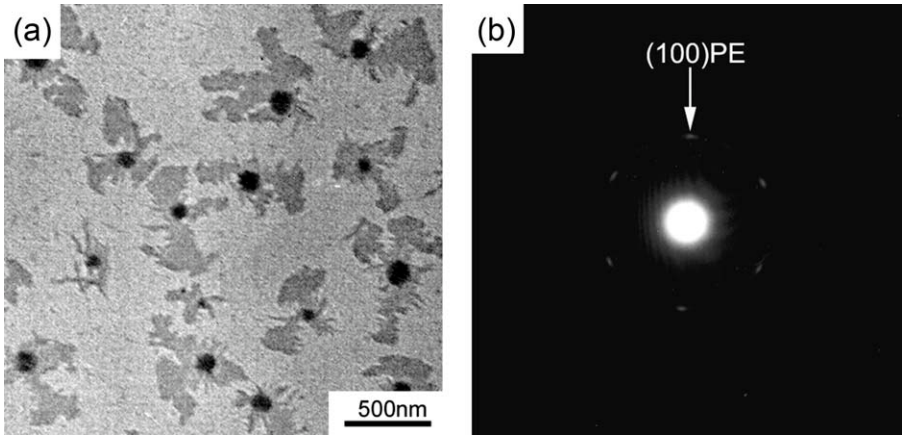

Figure 3 (a) TEM BF image of a solution-cast film of fraction F_c of hiPP; (b) SAED pattern of dark regions in (a).

PP crystals. We can see that PP crystals are always located in the periphery of PE phase. To prove whether these gray areas are PP homopolymer or copolymer, i.e., whether there exists a chemical bonding between PP and PE, we performed the diffraction. Analysis using SAED of the dark regions indicates that the PE crystals in these regions also exist in the hexagonal phase [Fig. 3(b)], which implies that PE in fraction F_c is not a homopolymer, but existing in a form of crystallizable ethylene-propylene copolymer. No electron diffraction pattern of PP homopolymer can be seen which further proves that PP is mainly in the form of copolymers and so F_c is composed of crystallizable ethylene-propylene copolymer.

Figure 4(a,b) show TEM BF images and corresponding electron diffraction pattern of a solution-cast film of fraction F_d, respectively, which display the morphological characteristic of PP homopolymer.

To further clarify the composition and chain structure of the four fractions of hiPP, especially the difference of crystallizable ethylene-propylene copolymers in both the fraction F_b and the fraction F_c, ^{13}C-NMR was utilized. The sequence distributions and the number-average sequence length of the blocks of PE and PP were derived from the calculation methods reported by Randall.[27] The results are summarized in Table II. For the fraction F_a, which is soluble in xylene at room temperature, both propylene and ethylene sequence distributions in all triads are relatively homogeneous (or broad) and their number-average sequence length is very short. These also demonstrate that the fraction F_a consists mainly of EPR. For the fraction F_c, which includes the soluble components in xylene in the temperature range of 80–100°C, both propylene and ethylene sequence distributions in all triads are very heterogeneous (or narrow). The amount of PPP and EEE is very high, whereas the number of transition segments (EPE and PEP) is much less. The molar contents of EPE and PEP are 0.2 and 0%, respectively. In addition, the number-average sequence length of propylene ($n_p = 337.0$) and ethylene ($n_E = 63.0$) sequences is much longer. These results, combined with the above morphological characterization, are convincing evidence that the fraction F_c is mainly composed of crystallizable

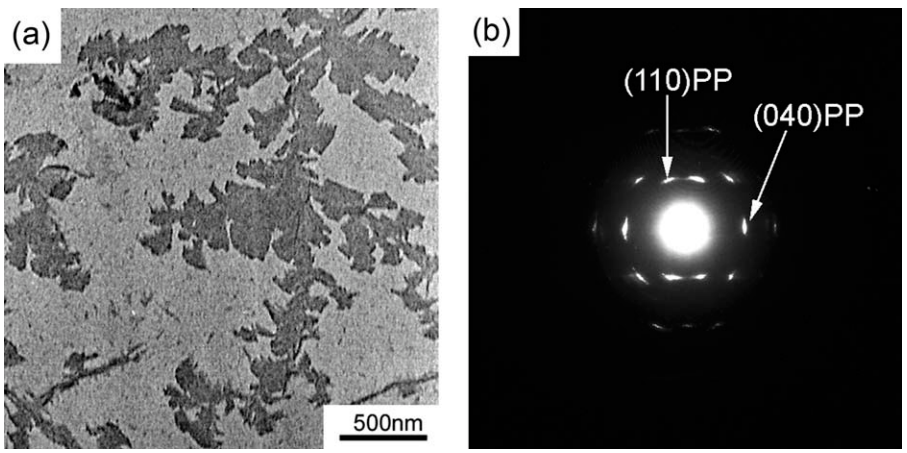

Figure 4 TEM BF image of a solution-cast film of fraction F_d of hiPP (a), and corresponding election diffraction pattern (b).

TABLE II
Composition and Chain Sequence Distribution of hiPP and its Fractions Based on ^{13}C-NMR

Samples	Molar composition (%)		Molar composition of the triads (%)						Number-average sequence length	
	P	E	PPP	PPE	EPE	EEE	PEE	PEP	n_P	n_E
F_a	53.2	46.8	25.1	19.3	8.8	19.4	17.3	10.1	2.8	2.5
F_b	55.0	45.0	47.1	4.9	3.0	36.4	6.3	2.3	10.1	8.2
F_c	84.3	15.7	83.3	0.8	0.2	15.2	0.5	0	337.0	63.0
F_d	100	0	100	0	0	0	0	0	–	–

ethylene-propylene block copolymer (PE-*b*-PP) though the block copolymer is not very pure. With respect to fraction F_b, which is the dissolved components at 80°C in xylene, the chain structure characteristic, including sequence distributions and number-average sequence length of PP and PE segments, is between that of fraction F_a and fraction F_c. In conjunction with the result of the above morphological characterization, we can draw a conclusion that the crystallizable copolymer in fraction F_b should be defined as ethylene-propylene segmented copolymer (PE-*s*-PP) with relatively short sequence length of PE and PP segments. With respect to fraction F_d, the insoluble part in xylene at 100°C is almost pure PP homopolymer.

Combining the morphological characterization results and the ^{13}C-NMR analysis, the composition and chain structure of various fractions of hiPP can be finally determined (Table III). Clearly, the high impact polypropylene used here contains at least five identifiable components, i.e., PP, EPR, PE-*b*-PP, PE-*s*-PP, and PE.

Relationship between chain structure and multiple phase morphology of hiPP

The complicated composition and chain structure must result in multiple phase morphology of hiPP. It is generally believed that the dispersed phase in hiPP exhibits a typical core-shell structure with PE core and EPR shell.[16–19] More recently, we observed a multilayered core-shell structure of the dispersed phase of hiPP in both the bulk and the solution cast film.[20,21]

Figure 5 shows the TEM BF electron micrograph of hiPP solution-cast film. Well-defined disperse phase particles, with diameter of ~ 0.2–0.5 μm, disperse uniformly in the PP matrix. The dispersed phases clearly demonstrate a multilayered core–shell morphology with inner core, intermediate layer, and outer shell (the dark ring).

Now the key point is how to identify the material composition of the multilayered core-shell structure of the dispersed phase in hiPP. Because of the limitations of small size and complex composition of the dispersed phase as well as current characterization method, it is very difficult or almost impossible to obtain structural details of the dispersed phase only from the dispersed phase itself. In this work, on the basis of chain structure characterization of various fractions, an unusual approach of selective remixing of different fractions of hiPP was adopted to clarify the material origin and composition of the multilayered core-shell structure of the dispersed phase, i.e., the different fractions of hiPP were selectively remixed by almost the same proportion compared with that of the original material.

Figure 6 shows the TEM BF electron micrographs of solution-cast films of the blends of different

TABLE III
Material Composition of Various Fractions of hiPP

Fraction	Composition
F_a (RT)	EPR, PP
F_b (80°C)	PE, PE-*s*-PP, PP
F_c (100°C)	PE-*b*-PP
F_d (>100°C)	PP

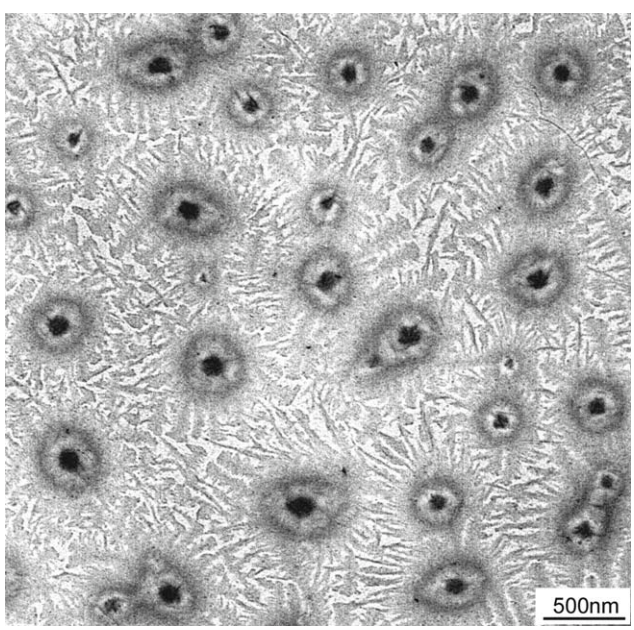

Figure 5 TEM BF image of a solution-cast film of hiPP, showing multilayered core-shell structure of the dispersed phases.

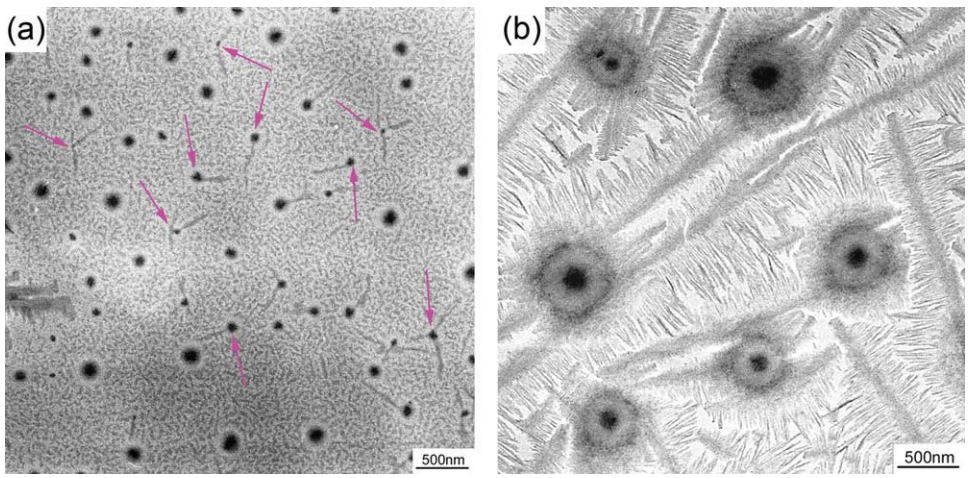

Figure 6 TEM BF images of solution-cast films of the blends of different fractions of hiPP: (a) $F_a/F_b/F_d = 26/5/69$, (b) $F_a/F_b/F_c/F_d = 26/5/7/62$. [Color figure can be viewed in the online issue, which is available at wileyonlinelibrary.com.]

fractions of hiPP. For $F_a/F_b/F_d = 26 : 5 : 69$ ternary blend [Fig. 6(a)], only a "simple" core-shell structure of the dispersed phase was observed. Clearly, the dark cores with strong contrast are polyethylene crystals resulting from PE and PE-*s*-PP in fraction F_b, and the bright shells with weak contrast come from EPR in fraction F_a. Examining the phase morphology carefully, it is found that some of the dark cores with relatively small size are connected with PP crystals (the gray lines), as shown by the arrows in Figure 6(a), which should be PE crystals resulting from PE-*s*-PP in fraction F_b, whereas the other dark cores of relatively large scale without connecting PP crystals represent the crystals of PE homopolymer. SAED provides further evidence that the dark regions exhibit two kinds of reflection patterns (the reflection patterns are omitted), corresponding to the reflections of orthorhombic and hexagonal phases of PE, respectively, as in the case of net fraction F_b (Fig. 2). This indicates clearly that, in the ternary blend, PE and PE-*s*-PP existing in fraction F_b form, respectively, individual cores. For $F_a/F_b/F_c/F_d = 26 : 5 : 7 : 62$ tetrad blend [Fig. 6(b)], the dispersed phase in solution-cast film displays clearly a multilayered core-shell structure similar to that of unfractionated hiPP sample. Unambiguously, the outer shell of the multilayered core-shell structure is PE crystals resulting from long PE blocks of PE-*b*-PP in fraction F_c. In this way, the material origin and composition of the multilayered core-shell structure of the dispersed phase in hiPP were clarified finally, i.e., the inner core is composed of PE-*s*-PP and PE, the intermediate layer is EPR, and the outer shell consists of PE-*b*-PP. Clearly, in addition to EPR and PE, the crystallizable ethylene-propylene copolymers, including PE-*b*-PP and PE-*s*-PP, play quite different roles in the formation of multiple phase morphology of hiPP.

The formation of the multiple phase morphology of hiPP results from the complexity of composition and chain structure as well as miscibility differences between various components in hiPP. For solution-cast films, during the solvent evaporation and film formation processes, the phase separations of PE and PE-*s*-PP as well as EPR took place first due to their immiscibility with PP matrix, which resulted in a simple core-shell structure formation of PE/EPR and PE-*s*-PP/EPR, as in the case of $F_a/F_b/F_d$ ternary blend [Fig. 6(a)]. This is similar to ordinary PP/EPR/PE ternary blend in which a core–shell morphology of PE core encapsulated by EPR shell is

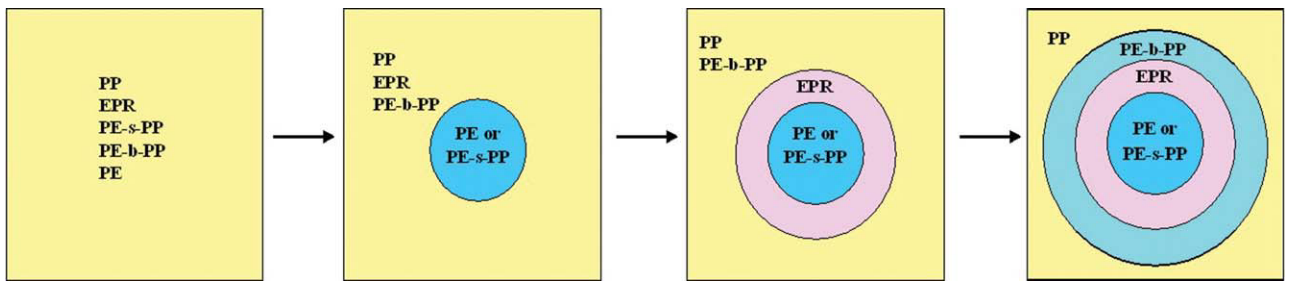

Figure 7 A schematic showing the formation process of the multilayered core-shell structure of the dispersed phase in hiPP. [Color figure can be viewed in the online issue, which is available at wileyonlinelibrary.com.]

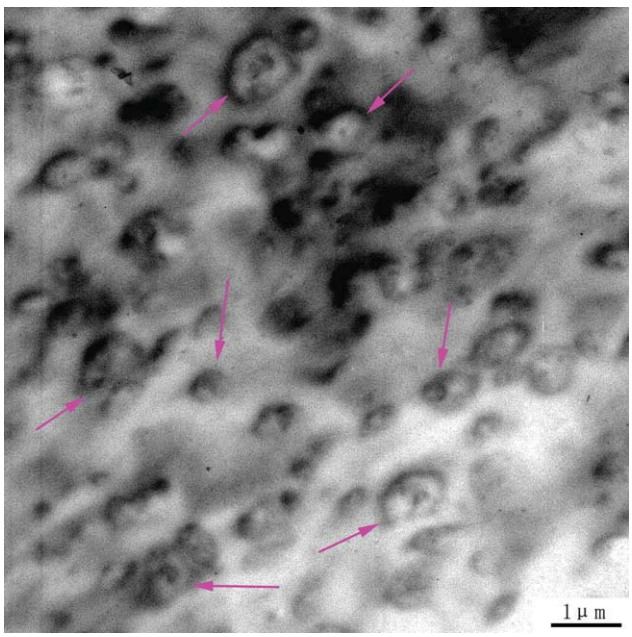

Figure 8 TEM BF image of a thin section of a hiPP pellet after melted at 200°C, showing multilayered core-shell structure of the dispersed phase. [Color figure can be viewed in the online issue, which is available at wileyonlinelibrary.com.]

usually formed.[28–30] Theoretical models based on interfacial Gibbs function and spreading coefficient can well explain this core-shell morphology formation.[30–32] In other words, interfacial interaction (or interfacial tension) between phases is a major factor that controls the phase structure.[33] The dominant morphology is the type with the lowest interfacial Gibbs function. However, the presence of PE-*b*-PP in hiPP made the phase structure of hiPP more complicated than that of simple PP/EPR/PE ternary blend. Because of the long PP block in PE-*b*-PP was highly miscible with the PP matrix, the PE-*b*-PP component in hiPP could not separate from the matrix at the early stage of the film formation. With further evaporation of the solvent and crystallization of the matrix PP, the long PE block in PE-*b*-PP, which was completely immiscible with PP, must be rejected from the matrix resulting in further phase separation of PE-*b*-PP with the PP matrix. Because the PE blocks in the block copolymer are compatible with the PE segments in EPR, the rejected PE-*b*-PP would be located at the periphery of previously formed PE/EPR (including PE-*s*-PP/EPR) core-shell dispersed phase, resulting in the formation of the outer-shell of the multilayered core-shell morphology of hiPP. Figure 7 is a schematic showing the formation process of the multilayered core-shell structure of the dispersed phase in hiPP.

It should be pointed out that a similar multilayered core-shell morphology of the dispersed phase in hiPP bulk was also observed. Figure 8 shows a TEM BF electron micrograph of a thin section of a hiPP pellet (The arrows indicate the dispersed phase particles with multilayered core-shell structure). It implies that this multistage phase separation process between different components of hiPP occurred in the melt processing process.[28] The fact that the two different preparation processes of solution-cast film and melt processing produce similar multilayered core-shell phase morphology is not a coincidence as the principle of phase separation and phase reorganization in the two processes are similar.

Unambiguously, the performances of hiPP are closely related to the multilayered core-shell structure of the dispersed phase. The soft intermediate layer EPR increases toughness, whereas the hard core and outer shell (mainly composed of PE crystals) can maintain high rigidity of the material.[34] It is known that interfacially active ethylene-propylene block copolymer can play the role of compatibilizer to enhance the interfacial adhesion between the EPR and PP phases.[6,7,17] Thus, the outer shell of the multilayered core-shell morphology of the dispersed phase in hiPP can be considered a compatibilizing layer bridging the EPR phase (the intermediate layer) with the PP matrix. In summary, it is the multiple phase morphology that makes the material have both the high toughness and the high rigidity.

CONCLUSIONS

The crystallizable ethylene-propylene copolymers, including PE-*s*-PP and PE-*b*-PP, play different and important roles in the formation of the multilayered core-shell structure of the dispersed phase of hiPP. PE-*s*-PP forms a hard inner core, which increases the rigidity of the dispersed phase. PE-*b*-PP results in a hard outer shell, which not only increases the rigidity of the dispersed phase but also enhances the adhesion between the dispersed phase with the PP matrix, making the material possess the mechanical properties of rigidity–toughness balance.

References

1. Galli, P.; Haylock, J. C. Prog Polym Sci 1991, 16, 443.
2. Debling, J. A.; Ray, W. H. J Appl Polym Sci 2001, 81, 3085.
3. Kittilsen, P.; Mckenna, T. F. J Appl Polym Sci 2001, 81, 1047.
4. Mirabella, F. M. Polymer 1993, 34, 1729.
5. Usami, T.; Gotoh, Y.; Umemoto, H.; Takayama, S. Polym Anal Charact 1993, 52, 145.
6. Cai, H.; Luo, X.; Ma, D.; Wang, J.; Tan, H. J Appl Polym Sci 1999, 71, 93.
7. Fan, Z.; Zhang, Y.; Xu, J.; Wang, H.; Feng, L. Polymer 2001, 42, 5559.
8. Xu, J.; Feng, L.; Yang, S.; Wu, Y.; Yang, Y.; Kong, X. Polymer 1997, 38, 4381.
9. Urdampilleta, I.; González, A.; Iruin, J. J.; de la Cal, J. C.; Asua, J. M. Macromolecules 2005, 38, 2795.
10. Feng, Y.; Hay, J. N. Polymer 1998, 39, 6723.
11. Sun, Z. H.; Yu, F. S.; Qi, Y. C. Polymer 1991, 32, 1059.

12. Cogswell, F. N.; Hanson, D. E. Polymer 1975, 16, 936.
13. Cecchin, G.; Marchetti, E.; Baruzzi, G. Macromol Chem Phys 1987 2001, 202.
14. McKenna, T. F.; Bouzid, D.; Matsunami, S.; Sugano, T. Polym React Eng 2003, 11, 177.
15. Cai, H.; Luo, X.; Chen, X.; Ma, D.; Wang, J.; Tan, H. J Appl Polym Sci 1999, 71, 103.
16. Radusch, H.; Doshev, P.; Lohse, G. Polimery (Warsaw) 2005, 50, 279.
17. Tan, H.; Li, L.; Chen, Z.; Song, Y.; Zheng, Q. Polymer 2005, 46, 3522.
18. Pegoraro, M.; Severini, F.; Di Landro, L.; Braglia, R.; Kolarik, J. Macromol Mater Eng 2000, 280/281, 14.
19. Ito, J.; Mitani, K.; Mizutani, Y. J Appl Polym Sci 1992, 46, 1221.
20. Chen, Y.; Chen, Y.; Chen, W.; Yang, D. C. Eur Polym Mater 2007, 43, 2999.
21. Chen, Y.; Chen Y.; Chen, W.; Yang, D. C. J Appl Polym Sci 2008, 108, 2379.
22. Bassett, D. C.; Block, S.; Piermarini, G. J. J Appl Phys 1974, 45, 4146.
23. Hu, W.; Srinivas, S.; Sirota, E. B. Macromolecules 2002, 35, 5013.
24. Bracco, S.; Comotti, A.; Simonutti, R.; Camutati, I.; Sozzani, P. Macromolecules 2002, 35, 1677.
25. Wright, K. J.; Lesser, A. J. Macromolecules 2001, 34, 3626.
26. Lieser, G.; Wegner, G.; Smith, J. A.; Wagener, K. B. Colloid Polym Sci 2004, 282, 773.
27. Randall, J. C. Polymer Sequence Determination; Academic Press: New York, 1977.
28. Petrović, Z. S.; Budinski-Simendić, J; Divjaković, V; Škrbić, Ź. J Appl Polym Sci 1996, 59, 301.
29. Ito, J.; Mitani, K.; Mizutani, Y. J Appl Polym Sci 1985, 30, 497.
30. Hemmati, M.; Nazokdast, H.; Panahi, H. S. J Appl Polym Sci 2001, 82, 1129.
31. Guo, H. F.; Packirisamy, S.; Gvozdic, N. V.; Meier, D. J. Polymer 1997, 38, 785.
32. Hobbs, S. Y.; Dekkers, M. E.; Watkins, V. H. Polymer 1988, 29, 1598.
33. Kopczynska, A.; Ehrenstein, G. W. J Mater Ed 2007, 29, 325.
34. Laupretre, F.; Bebelman, S.; Daoust, D. J Appl Polym Sci 1999, 74, 3165.